MICROWAVE HEATING AND FRACTURING CHARACTERISTICS OF BASALT
Insights from Infrared Thermal Imaging

by

Rui-Feng TANG [a,b]***, Ben-Gao YANG*** [a*]***, Zhu YANG*** [c]***,***
Yan-Bo BAI [a]***, and Hai-Chun HAO*** [a,b]

[a] State Key Laboratory of Intelligent Construction and Healthy Operation and Maintenance of Deep Underground Engineering, College of Civil and Transportation Engineering, Shenzhen University, Shenzhen, Guangdong, China
[b] State Key Laboratory of Intelligent Construction and Healthy Operation and Maintenance of Deep Underground Engineering, College of Water Resource and Hydropower, Sichuan University, Chengdu, Sichuan, China
[c] Northwest Engineering Co., Ltd., Xi'an, Shaanxi, China

Original scientific paper
https://doi.org/10.2298/TSC2502449T

Microwave heating is a promising assisted rock-breakage technology. However, the non-uniform temperature distribution in microwave-heated rocks has not been quantitatively studied. In this work, the microwave heating experiment with power ranging from 1.5-7.5 kW was conducted to investigate the fracturing and heating characteristics of basalt. The results show that the fracture time of basalt decreases non-linearly with increasing power, while the surface temperature increases linearly with irradiation time. For a fixed time, the uniformity of temperature distribution is more affected by power, while for a fixed input energy, the uniformity remains essentially unchanged. Increasing microwave power is more effective in enhancing the non-uniformity of temperature distribution and the increase of thermal stress.

Key words: *microwave heating, non-uniform temperature distribution, fracturing characteristics, basalt*

Introduction

The excessive consumption of primary energy on Earth necessitates the exploration of deep Earth as one of the effective ways to alleviate energy conflicts [1-3]. The high strength of deep rock mass leads to issues such as cutter wear, cutting failure, and reduced tunneling speed during mechanical excavation [4], significantly limiting the development and utilization of deep resources. Microwave technology, known for its high efficiency and environmental friendliness, is considered a promising assisted rock-breakage technology [5]. Using microwave pretreatment to weaken the mechanical properties of rocks could effectively improve excavation efficiency [6].

Essentially, the thermal effect of microwave is the primary reason for rock fragmentation. When the thermal stress induced by thermal mismatch and thermal gradient reaches the rock's ultimate tensile/shear strength, the fracture occurs [7, 8]. This is related to the mineralogy, spatial position, size, and water content of the heated material [9-12]. The study of the im-

[*] Corresponding author, e-mail: yangbgao@126.com

pact of microwave thermal effects on rock mechanical parameters is mostly conducted through laboratory experiments and numerical simulations. Pressacco *et al.* [13] conducted microwave treatment on granite through numerical simulation. The results showed that the main reason for the weakening of granite strength by microwave is the temperature increase. Kahraman *et al.* [9] conducted microwave treatment on nine types of igneous rocks and verified that strength loss depends on factors such as microwave power, irradiation time, and mineralogy, which affect the heating degree of igneous rocks. Ahmadihosseini *et al.* [14] found that the real part of the dielectric constant changes the temperature distribution in basalt. At the same output energy, higher power generates higher temperature in the samples, which is beneficial for rock fracturing. Meanwhile Sun *et al*. [15] quantitatively described the relationship between granite fracturing and temperature using infrared monitoring.

The aforementioned studies have promoted the research on the characteristics and mechanisms of microwave-assisted rock breakage under microwave thermal effects. However, there is still a lack of quantitative research on the non-uniform temperature distribution characteristics of basalt in a multimode applicator, and the mechanism of microwave-induced rock fracturing needs further exploration from a temperature perspective. Therefore, the purpose of this work is to quantitatively investigate the temperature distribution characteristics of basalt, revealing the mechanism of microwave-induced rock fracturing from the perspective of microwave thermal effects, thus providing a theoretical basis for the efficient development of deep resources.

Experiment method and procedure

Material properties and sample preparation

The rock material used in this work is basalt, sourced from Guangdong Province, China. All specimens were taken from the same rock mass and processed into standard cylindrical specimens of ∅50 mm × 100 mm. The orthogonal polarized light microphotograph is shown in fig. 1. Petrographic analysis revealed that the mineral composition of the basalt is 37% pyroxene, 59% plagioclase, and 2% olivine. It has a density of 2710 kg/m^3, a *P*-wave velocity of 5556 m/s and a uniaxial compressive strength of 207.7 MPa.

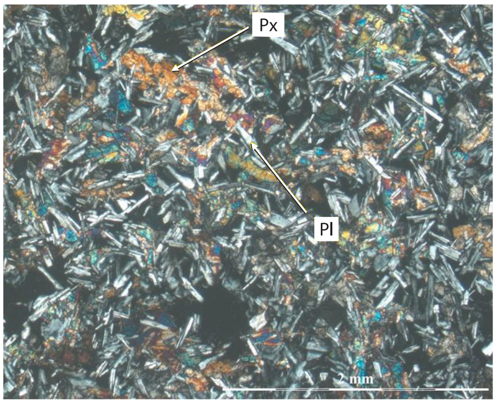

Figure 1. Petrographic microphotograph of basalt: *Px – pyroxene and Pl – plagioclase*

Testing system and scheme design

The microwave experiment was conducted using a self-developed industrial microwave testing system, as shown in fig. 2, with an adjustable output power of 0-15 kW and an output frequency of 2.45 GHz. The testing system consists of a microwave power supply, microwave generator, WR340 waveguide, impedance tuner, water load, and multimode cavity applicator.

To study the effect of microwave power on the temperature characteristics of basalt, microwave heating tests were conducted on the specimens with power ranging from 1.5-7.5 kW. The microwave irradiation was stopped when the camera observed molten minerals on the specimen surface. It should be noted that before the microwave experiment, the specimens were subjected to a drying treatment, where the specimens were continuously dried at 80 °C for 48 hours in a constant temperature drying oven to eliminate the effect of open pore water on microwave heating.

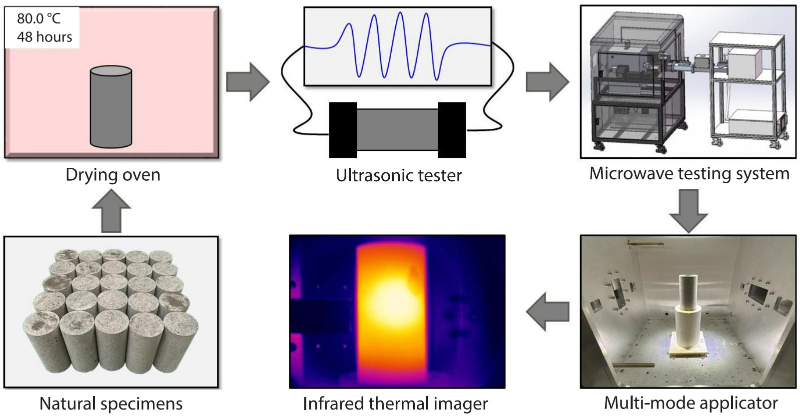

Figure 2. Testing devices and procedures

Results and discussion

Basalt fracturing and heating characteristics in microwave field

The fracture results of basalt under different microwave power are shown in fig. 3(a). Therefore, based on the observed melt phenomena, the fracture times of the specimens at different power levels were 677 seconds, 178 seconds, 106 seconds, 68 seconds, and 50 seconds. With the increase in microwave power, the fracture times decreased by 73.71%, 40.45%, 35.85%, and 26.47%. The most significant reduction in fracture time occurred when the power increased from 1.5-3 kW, after which the rate of reduction gradually slowed, showing a non-linear trend. Overall, when the microwave power increased from 1.5-7.5 kW, the fracture time of basalt was reduced by a total of 92.61%.

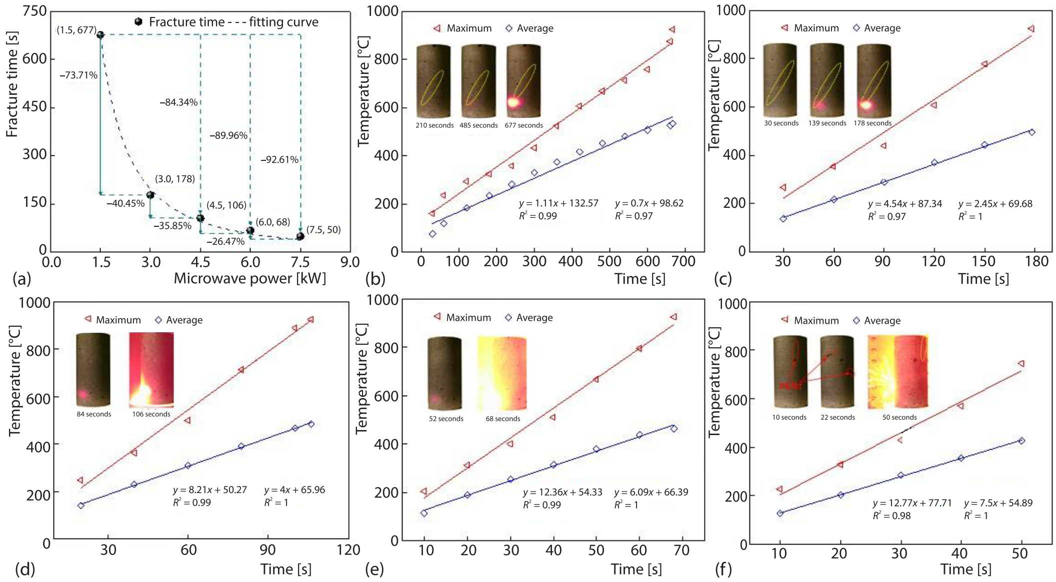

Figure 3. Fracturing and heating results of basalt;
(a) fracture time, (b) 1.5 kW, (c) 3.0 kW, (d) 4.5 kW, (e) 6.0 kW, and (f) 7.5 kW

The heating characteristics of basalt is shown in figs. 3(b)-3(f). Overall, the surface temperature shows an approximately linear growth trend. Under 1.5 kW, the maximum and average temperature initially rose rapidly, slowed down after 120 seconds, and showed a steep increase after 600 seconds, which is related to the appearance of molten minerals. At 210 seconds, surface microcracks were observed, and it is speculated that the fluctuation in heating rate is related to the evaporation of internal pore water carrying away heat. Before the final fracturing, the monitored maximum and average temperature were 924.9 °C and 534.8 °C, with heating rate of 1.11 °C per seconds and 0.7 °C per seconds. Under 3.0 kW, the maximum and average temperature were 924.9 °C and 496.3 °C, with heating rate increasing to 4.54 °C per seconds and 2.45 °C per seconds. Microcracks appeared on the surface at 30 seconds and further developed thereafter. Under 4.5 kW and 6.0 kW, molten minerals flowed out from the bottom of the specimens, but the heating rate was as high as 12.36 °C per seconds at 6.0 kW and 8.21 °C per seconds at 4.5 kW, with no microcracks observed on the surface. Under 7.5 kW, the specimen thermal responded most violently, with molten minerals almost splashing out. Evaporation of water was observed just 10 seconds after microwave irradiation, and the evaporation sites coincided with the crack locations, indicating that water promotes in promoting crack formation. The surface temperature was 746.2 °C and 426.8 °C, with heating rate of 12.77 °C per seconds and 7.5 °C per seconds. The maximum heating rate did not significantly increase compared to 6.0 kW, further indicating that the thermal sensitivity of basalt to high power microwave mainly occurs inside the basalt.

In addition, it could be observed that the locations of molten minerals in basalt are consistent at different power levels, all situated in the middle to lower part of the specimens, indicating that when the rock type is determined, the electric field distribution characteristics in the applicator are basically the same. As the microwave power increases, the forms in which molten minerals appear could be categorized as calm, flowing out, and splashing. These phenomena to some extent reflect the magnitude of thermal stress generated after mineral phase transformation.

Uniformity of temperature distribution

To quantify the non-uniformity of the basalt temperature distribution, the temperature coefficient of variation, COV_T, was utilized. This coefficient reflects the internal damage to a certain extent:

$$COV_T = \frac{1}{\overline{T}}\sqrt{\frac{1}{N}\sum_{i=1}^{N}\left(T_i - \overline{T}\right)^2} \tag{1}$$

where T_i is the temperature at a point, $\overline{T}$ – the average temperature, and N – the number of points. A higher COV_T value indicates a more non-uniform temperature distribution.

The evolution of COV_T values of basalt under different power levels is shown in fig. 4. When $t = 30$ seconds, with the increase of microwave power, the COV_T value first increased and then decreased, reaching a maximum of 0.43 at 3 kW, and only 0.23 kW at 7.5 kW. When the power exceeded 4.5 kW, the trend of COV_T change significantly slowed down. When the microwave output energy was 225 kJ, the COV_T value still maintained the trend of first rising and then falling, but the maximum difference is only 0.05. When the power exceeded 4.5 kW, the COV_T value basically no longer changed. The COV_T value of 3 kW was still the highest, at 0.28, but the difference from the COV_T values under other conditions was tiny. As the irradiation time increased, the COV_T value showed a *V* shaped trend. The change in COV_T value could be explained by three reasons: First, due to the influence of convective heat transfer with air and heat transfer between minerals, the temperature distribution tended to become uniform, causing the COV_T value to decrease. Second, the evaporation of pore water carried away part of the heat, increasing the uniformity of temperature distribution and causing the COV_T value to decrease. Third, the mineral phase transformation, where the outflow of molten minerals caused a significant rise in regional temperature, increased the non-uniformity of temperature distribution and caused the COV_T value to increase.

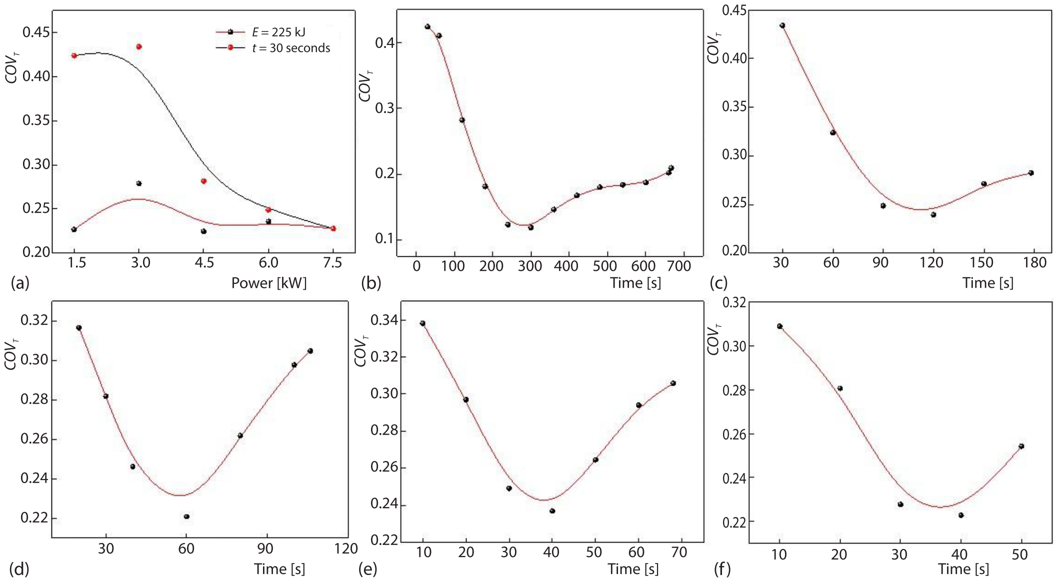

Figure 4. Coefficient of variation evolution law of basalt; (a) power, (b) 1.5 kW, (c) 3 kW, (d) 4.5 kW, (e) 6.0 kW, and (f) 7.5 kW

The uneven distribution of the electric field in the applicator caused significant hot and cold zone effects on the surface of basalt, as shown in fig. 5. When the irradiation time is 30 seconds, an increase in microwave power leads to a greater range of temperature non-uniformity. The reason is that as microwave power increased, the heating rate of the specimen significantly increased, creating more new cracks within the same time. These cracks acted as channels for water to escape, carrying away a large amount of heat from the hot zone, which is the main reason for the decrease in the COV_T value from 3.0-4.5 kW.

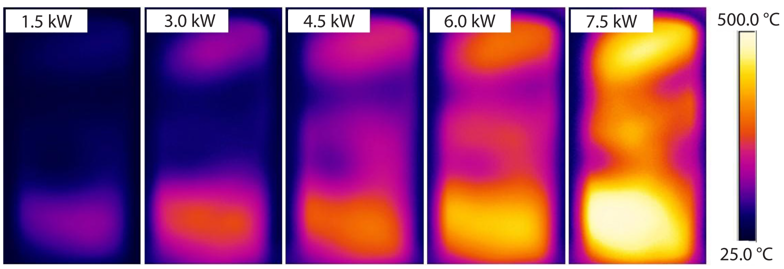

Figure 5. Infrared images of basalt heated for 30 seconds

Conclusion

Based on the infrared thermal imager, the non-uniform temperature distribution characteristics of basalt in the microwave field were quantitatively revealed. As microwave power increases from 1.5-7.5 kW, the fracture time of basalt decreases non-linearly, with a total reduction of 92.61%. The surface temperature has a linear relationship with the irradiation time. The temperature uniformity is mainly influenced by the distribution of the electric field, water, and heat transfer. When the irradiation time is constant, the uniformity value is more affected by microwave power. For the fixed input energy, there is no significant difference in temperature distribution uniformity.

Acknowledgment

This work was financially supported by Sichuan Science and Technology Program (2023NSFSC0004), National Natural Science Foundation of China (52225403, 42407249, U2013603), and China Postdoctoral Science Foundation (2024M762221).

Nomenclature

T_i – temperature at a point, [°C]

T – average temperature, [°C]

References

[1] Gao, M. Z., *et al*., The Mechanism of Microwave Rock Breaking and Its Potential Application Rock-Breaking Technology in Drilling, *Petroleum Science*, *19* (2022), 3, pp. 1110-1124
[2] Tang, M. Y., *et al*., Failure Behavior and Energy Evolution Characteristics of Deep Roadway Sandstone under Different Microwave Irradiation Modes, *Journal of Central South University, 30* (2023), 1, pp. 214-226
[3] Gao, M. Z., *et al*., Fractal Evolution and Connectivity Characteristics of Mining-induced Crack Networks in Coal Masses at Different Depths, *Geomechanics and Geophysics for Geo-Energy and Geo-Resources*, *7* (2021), 1, ID9
[4] Zheng, Y. L., *et al*., Challenges and Opportunities of Using Tunnel Boring Machines in Mining, *Tunnelling and Underground Space Technology*, *57* (2016), 8, pp. 287-299
[5] Yang, B. G., *et al*., Exploration of Weakening Mechanism of Uniaxial Compressive Strength of Deep Sandstone under Microwave Irradiation, *Journal of Central South University*, *29* (2022), 2, pp. 611-623
[6] Lu, G. M., *et al*., Influence of Microwave Treatment on Mechanical Behaviour of Compact Basalts under Different Confining Pressures, *Journal of Rock Mechanics and Geotechnical Engineering, 12* (2020), 2, pp. 213-222
[7] Li, J. L., *et al*., Fully-Coupled Simulations of Thermally-induced Cracking in Pegmatite due to Microwave Irradiation, *Journal of Rock Mechanics and Geotechnical Eng.*, *11* (2019), 2, pp. 242-250
[8] Toifl, M., *et al*., Numerical Study of the Influence of Irradiation Parameters on the Microwave-Induced Stresses in Granite, *Minerals Engineering*, *103* (2017), 4, pp. 78-92
[9] Kahraman, S., *et al*., The Influence of Microwave Treatment on the Compressive and Tensile Strength of Igneous Rocks, *International Journal of Rock Mechanics and Mining Sciences*, *129* (2020), 5, ID104303
[10] Pressacco, M., *et al*., Numerical Modelling of Microwave Heating Assisted Rock Fracture, *Rock Mechanics and Rock Engineering*, *55* (2022), 2, pp. 481-503
[11] Zhao, Q. H., *et al*., Microwave Fracturing of Water-bearing Sandstones: Heating Characteristics and Bursting, *International Journal of Rock Mechanics and Mining Sciences*, *136* (2020), 12, ID104495
[12] Hassani, F., *et al*., The Influence of Microwave Irradiation on Rocks for Microwave-assisted Underground Excavation, *Journal of Rock Mechanics and Geotechnical Engineering*, *8* (2016), 1, pp. 1-15
[13] Pressacco, M., *et al*., Numerical Modelling of Microwave Irradiated Rock Fracture, *Minerals Engineering*, *203* (2023), 11, ID108318
[14] Ahmadihosseini, A., *et al*., Computational Study of Microwave Heating for Rock Fragmentation, Model Development and Validation, *International Journal of Thermal Sciences*, *181* (2022), 11, ID107746
[15] Sun, T. W., *et al*., Microwave Heating and Fracturing of Granite: Insights from Infrared Thermal Imaging, *Journal of Thermal Stresses*, *45* (2022), 9, pp. 762-771

Paper submitted: October 4, 2024
Paper revised: November 13, 2024
Paper accepted: November 22, 2024